ISSN 1726-5479

SENSORS & TRANSDUCERS

vol. 101
2/09

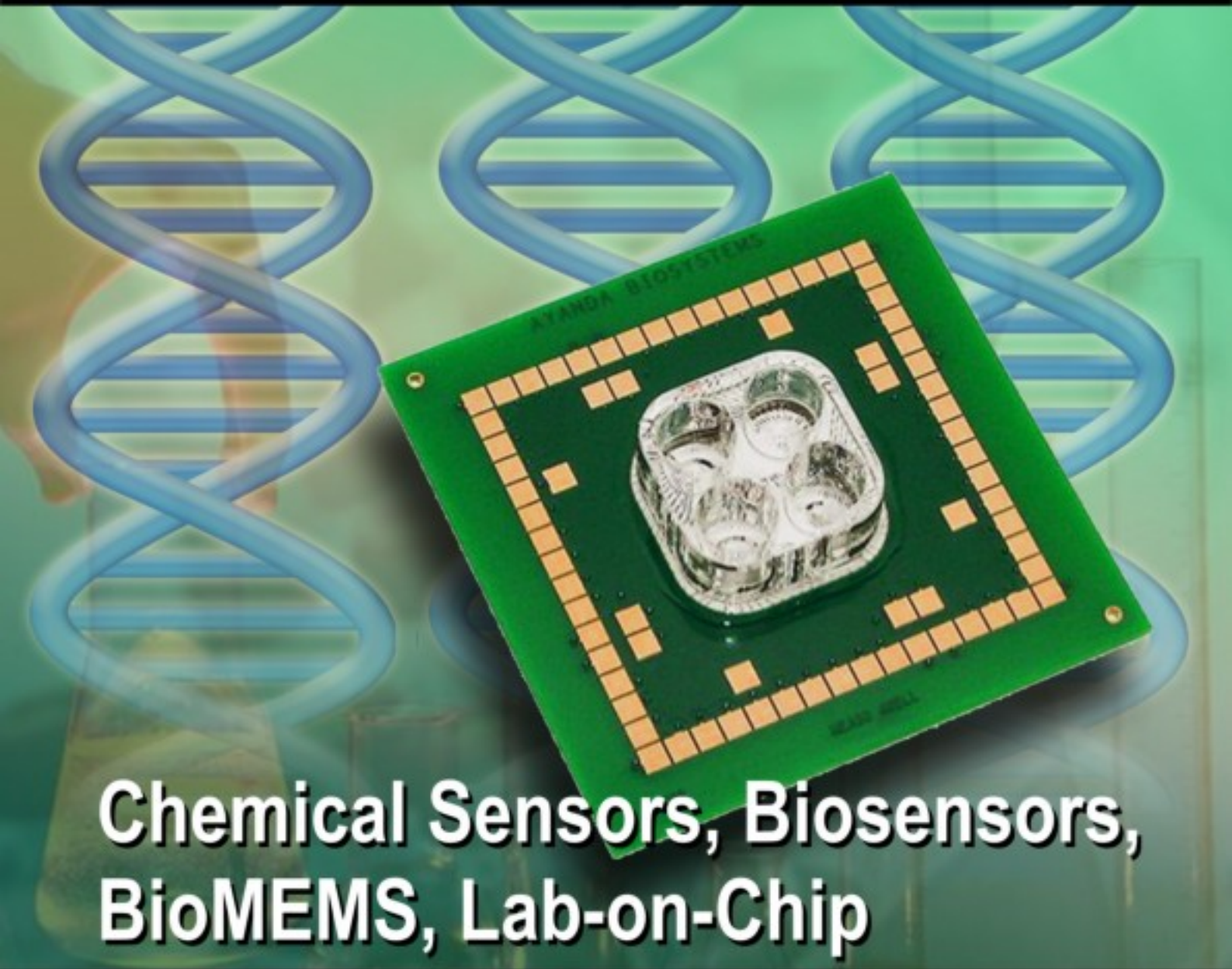

Chemical Sensors, Biosensors, BioMEMS, Lab-on-Chip

International Frequency Sensor Association Publishing

IFSA

Sensors & Transducers

Volume 101
February 2009

www.sensorsportal.com

ISSN 1726-5479

Sensors & Transducers Journal (ISSN 1726-5479) is a peer review international journal published monthly online by International Frequency Sensor Association (IFSA).
Available in electronic and CD-ROM.

Sensors & Transducers Journal

Contents

Volume 101
Issue 2
February 2009

www.sensorsportal.com

ISSN 1726-5479

Research Articles

Authors are encouraged to submit article in MS Word (doc) and Acrobat (pdf) formats by e-mail: editor@sensorsportal.com
Please visit journal's webpage with preparation instructions: http://www.sensorsportal.com/HTML/DIGEST/Submition.htm

Sensors & Transducers Journal, Vol. 101, Issue 2, February 2009, pp. 132-151

www.sensorsportal.com

Sensors & Transducers

ISSN 1726-5479

http://www.sensorsportal.com

Non-invasive Blood Glucose Quantification Using a Hybrid Sensor

[1]Sundararajan JAYAPAL, [2]Dr. V. Palanisamy, [1]Sandeep MANDYAM
Anna University, Chennai
[1]Paavai Engineering College, NH-7, Pachal, Namakkal-637 018
[2]Info Institute of Engineering, Coimbatore-641107
Tamilnadu, India
E-mail: Dharsini_71@yahoo.co.in, Mandyam_sandeep@yahoo.co.in

Received: 26 November 2008 /Accepted: 20 February 2009 /Published: 28 February 2009

Abstract: Diabetes Mellitus is a group of metabolic diseases characterized by high blood sugar (glucose) levels which result from defects in insulin secretion. It is very important for the diabetics and normal people to have a correct blood glucose level. The HbA1c test is the most preferred test by renowned doctors for glucose quantification. But this test is an invasive one. At present, there are many available techniques for this purpose but these are mostly invasive or minimally non-invasive and most of these are under research. Among the different methods available, the photo acoustic (PA) methods provide a reliable solution since the acoustical energy loss is much less compared to the optical or other techniques.

Here a novel framework is presented for blood glucose level measurement using a combination of the HbA1c test and a PA method to get an absolutely consistent and precise, non-invasive technique. The setup uses a pulsed laser diode with pulse duration of 5-15 ns and at a repetition rate of 10 Hz as the source. The detector setup is based on the piezoelectric detection. It consists of a ring detector that includes two double ring sensors that are attached to the ring shaped module that can be worn around the finger. The major aim is to detect the photo acoustic signals from the glycated hemoglobin with the least possible error.

The proposed monitoring system is designed with extreme consideration to precision and compatibility with the other computing devices. The results obtained in this research have been studied and analyzed by comparing these with those of in-vitro techniques like the HPLC. The comparison has been plotted and it shows a least error. The results also show a positive drive for using this concept as a basis for future extension in quantifying the other blood components. *Copyright © 2009 IFSA.*

Keywords: Photo acoustic (PA), HbA_{1C}, Pulsed repetition frequency, Pulsed laser diode, Double ring sensor, Direction sensitivity

1. Introduction

Diabetes is a serious disorder of the glands, of pancreas to be exact. It is one of the most insidious disorders of the metabolism and, if left undiagnosed, may lead to rapid emaciation and ultimately death. The measurement of the total glycated hemoglobin concentration is the widely used blood test for quantifying glucose in normal as well as diabetic patients. The reason for this is the versatile nature of this molecule. The complications associated with diabetes are mainly due to the non-enzymatic glycation of proteins [2, 17, 24, 27]. The Maillard hypothesis suggests that chemical modification of proteins by glucose and subsequent reactions of the adduct may result in products which are directly responsible for many pathological conditions in diabetes [2, 3, 12]. The reaction of glucose with amino groups in proteins results in the reversible formation of a Schiff's base or aldimine, which can undergo irreversible Amadori rearrangement (Fig. 1) to form a ketoamine product. Glycation is also a process that appears to be associated with age-related disorders and may be particularly important in the context of long-lived proteins which do not undergo rapid synthesis and turnover [15, 24]. The purpose of many such studies was the characterization of site-specificity of glycation and the factors catalyzing rearrangement to the Amadori product. At present, the technique for quantifying HbA_{1C} (glycated hemoglobin) concentration is invasive and cannot provide results rapidly. Here we propose to use a photo acoustic technique for non-invasive and accurate measurement of HbA_{1C} concentration.

The photo acoustic technique is based on the generation of a near infrared wave by pulsed laser diode and time-resolved detection of the acoustical wave by the acoustical transducer. It can be used for tissue characterization with high contrast (photo acoustic signal parameters are dependent on the optical properties of the irradiated tissue) and high resolution due to time-resolved detection of acoustic waves. Since hemoglobin A1C (HbA_{1C}) is the post translational modification of glucose and hemoglobin, the major blood component, the photo acoustic technique is sensitive to variation of its concentration. The glucose molecules in the blood attach themselves to many of the chemical compounds like hemoglobin, low density lipoprotein (LDL's), serum proteins (like albumin) and many more. When it is in the free aldehyde form, it can react with the hemoglobin molecule within the red cells of blood to form an aldimine adduct as shown in the Fig. 1. But this is a reversible reaction in equilibrium with the blood glucose and hence this aldimine adduct is labile. However it can undergo a shift in the double bond to the second carbon in an "Amadori Rearrangement" [20] to form a ketoamine adduct as shown.

This ketoamine adduct is an irreversible arrangement of the hemoglobin and glucose molecules. The optical absorption spectra and the photo acoustic spectra of the free glucose and hemoglobin, the aldimine and the ketoamine are each sufficiently different to form the basis for spectroscopic determination of the amounts of each form present in the blood. Now HbA_{1C} is the most prevalent of the ketoamine adducts with the β chain of the hemoglobin, representing 5 to 6% of the total hemoglobin in persons without diabetics. This gives the justification for the choice of HbA1c for glucose quantification.

Apart from the individual demerits, the invasive methods [22, 23] have a common drawback that they cause pain and inconvenience to the patient. In view of the fact that the main aim of the in vivo technique is to create a patient-friendly system, the invasive systems can well be crossed out. Arriving at the non-invasive and minimally invasive methods of glucose level measurement there are a lot of techniques in the developmental phase and research is extensively being done in this area. Some of these existing techniques are described briefly.

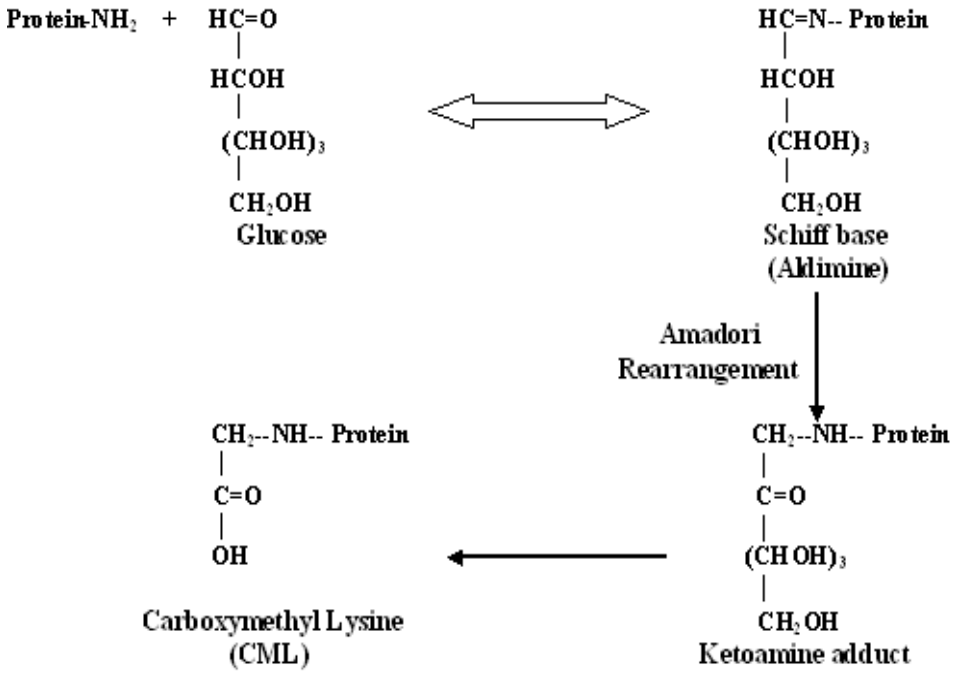

Fig. 1. Amadori Rearrangement.

1.1. Near Infra-Red Spectroscopy

NIR spectroscopy [8] has been a regular choice for the study of the glucose measurement. But the main difficulties with this technique are the large absorption values of water, and the similar absorption behavior of proteins and non-glucose metabolites. The key problem is that the spectral variations due to glucose concentration are extremely small compared to that from other biological components.

1.2. Near Infrared Diffuse-Reflectance Spectroscopy

This is also a popular field of research which utilizes the reflectance properties of NIR. The problem of light scattering, diffusion [7, 13] and absorbance interferes with this technique causing errors and another drawback is that separate calibration models should be used for each person in the tests.

1.3. Thermal Emission Spectroscopy

Thermal infrared vibrational spectroscopy is based on the principle that vibrational motions occur within a crystal lattice at fundamental frequencies that are directly related to the crystal structure and elemental composition [10, 16, 29]. The device setup in this technique has demonstrated only a reasonable accuracy of measurement in glucose with the mean absolute relative error at 11.6% for which alternate techniques can be preferred.

1.4. Raman Spectroscopy

Raman spectroscopy [30] offers the possibility of remotely obtaining a measurement of glucose in vivo because, in contrast to infrared spectroscopy, its spectral signature is not obscured by water. In addition, Raman spectral bands are considerably narrower than those produced in classical infrared

spectral experiments and Raman excitation in the near infrared region (700-1300 nm) encounters minimal fluorescence in aqueous media. It is relatively inexpensive, but there is a problem with noise in the signal and it is currently under developmental phase.

The HbA1c test is briefly explained here. The Hb_{A1C} test is a valuable measure of the overall effectiveness of blood glucose control over a period of time. The percentage of glycated hemoglobin in the blood and its interpretation in terms of glucose levels is given in the Table 1. In individuals with poorly controlled diabetes, increases in the quantities of these glycated hemoglobins are noted.

Table 1. Relationship of A1C to Average Whole Blood and Plasma.

HbA1c %	Mean Blood Glucose (mg/dL)	Average Plasma Glucose	Interpretation
4	61	65	Non-Diabetic Range
5	92	100	
6	124	135	
7	156	170	Target for Diabetes in Control
8	188	205	Action Suggested according ADA guidelines
9	219	240	
10	251	275	
11	283	310	
12	314	345	

The Hb_{A1c} level is proportional to average blood glucose concentration over the previous four weeks to three months. The glycated hemoglobin test gives accurate glucose measurements to maximum extent since the concentration of glucose in the blood is proportional to the extent of glycosylization of the hemoglobin. In most labs, the normal range is 4-5.9 %. In poorly controlled diabetes, its 8.0% or above, and in well controlled patients it's less than 7.0%. The benefits of measuring Hb_{A1c} is that is gives a more reasonable view of what's happening over the course of time (3 months), and the value does not bounce as much as finger stick blood sugar measurements. But the disadvantage of the Hb_{A1c} test is that the normal values for the glycated hemoglobintest may vary from laboratory to laboratory because different laboratories use different procedures to perform themeasurement. As a result of this diabetics may be restricted to taking their test only from a particular lab affecting their professional schedules or the diabetics may have to include their medical reports along with the documentary and carry it around, everywhere.

2. Photo Acoustic Methods

As mentioned, a combination of photo acoustic methods and the HbA1c test has been used here. Photo acoustics has many applications [9, 18] and bio medical engineering is one particular area that has taken photo acoustics into deep consideration. The following sections describe the methods and the designs involved in this work.

2.1. Generation of Photo Acoustic Waves

Among all the sources, the modulated light energy is used in this paper to generate PA waves. This is because light consists of non-ionizing radiation, which is not harmful to the human body, and there are abundant, economical and effective optical sources and devices. The various mechanisms capable of generating PA waves are shown in Fig. 2.

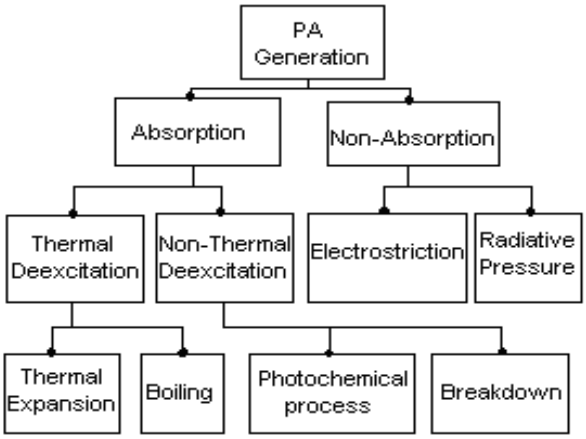

Fig. 2. Different PA generating mechanisms.

The chief principle that is used in the PA mechanism is the optical absorption followed by thermal de-excitation. The basis for using thermal expansion from among various other mechanisms in the glucose quantification is that it does not break or change the properties of the object under study. It also has a linear or a definite relationship with many of the physical parameters of diverse materials and it is non-destructive or non-invasive in application such as materials test and medial diagnosis.

2.2. Thermal Expansion

The in progress technique would employ high peak power pulsed laser diodes which are compact, relatively inexpensive, and available in a wide variety of NIR wavelengths as excitation sources. When the light from these laser diodes irradiates the skin and tissues (absorbing medium), the ion specific absorption in the illuminated region produces heat due to non-radiative relaxation. This heat causes the region to expand. If the pulse duration of the laser is short enough or its modulated frequency rapid enough, the thermal expansion will be exceedingly fast. Due to this action, an acoustic wave is generated and propagated outside. This wave is subsequently detected by an acoustic transducer. The amplitude of the acoustic wave is linearly proportional to the absorbed energy density, while the shape of the wave is dependent on the absorption distribution, laser parameters and boundary condition. The thermal elastic direct PA generation by pulsed excitation mode will be the PA technique used in the *in vivo* technique that is being discussed.

2.3. Excitation System - High-Peak Power Pulsed Laser Diodes

For an effective generation of PA signals, laser pulse durations in the range of tens to hundreds of nanoseconds are required. Also to acquire sufficient penetration depth, the near infrared (NIR) range (600–1200 nm) should be used as at such a wavelength the biological tissues are pretty translucent. The high peak power pulsed laser diode system is used in preference than the typical Q-switched Nd: YAG laser. Comparatively the pulsed laser diode system is economical with simpler driver electronics apart from giving a wide range of NIR wavelengths.

3. The Detector Design

The design of the detector module has been explained in detail in the following sections. It has two double ring sensors as components whose design is also explained.

3.1. Piezoelectric Constants

A piezoelectric ceramic is anisotropic and hence the physical constants relate to both the direction of the applied mechanical or electric force and the directions perpendicular to the applied force. Consequently, each constant generally has two subscripts that indicate the directions of the two related quantities, such as stress (force on the ceramic element / surface area of the element) and strain (change in length of element / original length of element) for elasticity (Fig. 3).

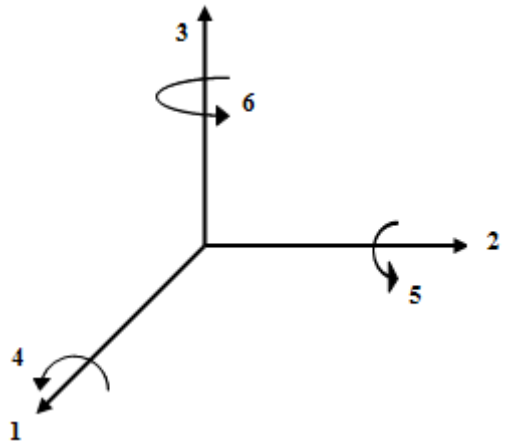

Fig. 3. Illustration of the piezoelectric constants.

The direction of positive polarization usually is made to coincide with the Z-axis of a rectangular system of X, Y, and Z axes. Direction X, Y, or Z is represented by the subscript 1, 2, or 3, respectively, and shear about one of these axes is represented by the subscript 4, 5, or 6, respectively. The piezoelectric charge constant, d, the piezoelectric voltage constant, g, and the permittivity, e, are temperature dependent factors [6].

3.2. Sensor Design

The opening angle for a sensor is defined as the angle of incidence of ultrasound with respect to the normal of the sensor surface at which the amplitude of the generated voltage is decreased to half of the maximum value. To monitor local blood content in tissue, at depths up to about 3 cm, a sensor is required, which is sensitive only to variations in blood content, which occur on a line in depth. This implies that this sensor should have a very small opening angle. The shape and size of the piezoelectric element determines the characteristics of the sensor, such as the opening angle. The directional sensitivity and depth response to a spherical photo acoustic source can be calculated to characterize a sensor. The depth response is defined as the signal maximum as a function of depth of the source, while the source is located on-axis. The directional sensitivity is the signal maximum as a function of the lateral displacement of the source for a certain depth. Depth response is defined as response of the sensor to an acoustic point source located on-axis (x=0) as a function of depth z. Directional sensitivity is defined as response of the sensor to an acoustic source located at a fixed depth z, as a function of the off-axis position x of the source. Direction sensitivity and depth response of a sensor are depicted in Fig. 4.

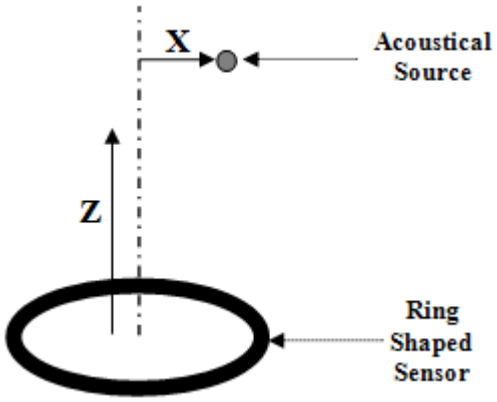

Fig. 4. Direction sensitivity and depth response.

A spherical photo acoustic source with a Gaussian absorption distribution (1/e radius r0), homogeneously illuminated, will generate a spherical pressure wave, which at a distance r (r>>r0) from the source at time t can be described by

$$P(r,t) = -P_{max}(r)\sqrt{e}\frac{t-\tau}{\tau_e}\exp\left\{-\frac{1}{2}\left(\frac{t-\tau}{\tau_e}\right)^2\right\}; \quad (1)$$

$$P_{max}(r) = \frac{\beta E_a}{2\sqrt{e}(2\pi)^{3/2}C_p\tau_e{}^2 r};\ \tau = \frac{r}{v};$$

$$\tau_e = \sqrt{\tau_a^2+\tau_1^2};\quad \tau_a = \frac{\frac{1}{2}\sqrt{2}r_0}{v},$$

where β is the thermal expansion co-efficient [K^{-1}], C_p is the specific heat capacity [J/kg.K], τ1 is half the pulse duration between the 1/e-points of the temporal amplitude distribution of the laser pulse [s], and Ea is the amount of laser pulse energy which is absorbed by the photo acoustic source [J].

3.3. The Sensor Width

The width of the ring is an important parameter in the design of a ring sensor. For optimal charge generation, the maximum path length difference for the acoustic signals, arriving at the ring shaped sensor, should be smaller than a quarter of the acoustic wavelength, determining the maximum width (w) of the ring shaped sensor.

$$\sqrt{z^2+(R+w)^2}-\sqrt{z^2+R^2} \le \lambda/4, \quad (2)$$

where z = depth of photo acoustic source.
R = inner radius of ring shaped sensor surface
w = width of ring shaped sensor surface.

Fig. 5 gives the maximum width of the ring for various inner ring radii as a function of depth for photo acoustic sources with peak to peak times of 25 ns. It is obvious that with increasing peak to peak time

the maximum width increases. The maximum width of the ring is determined by the minimum depth at which the photo acoustic signal has to be detected with maximum charge generation.

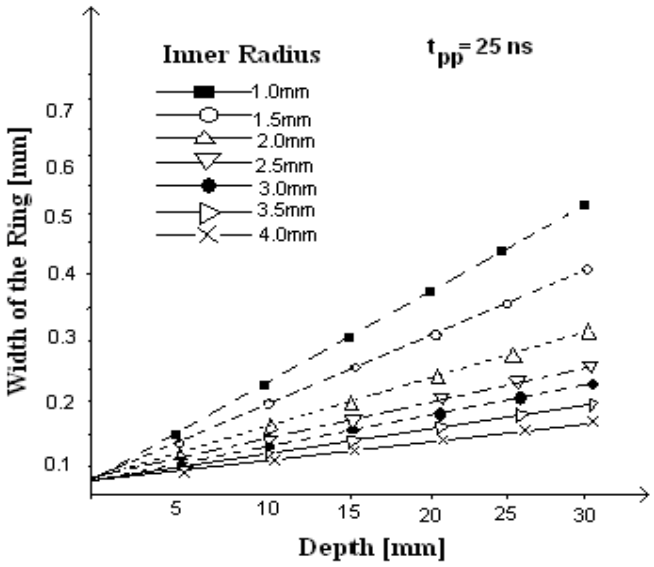

Fig. 5. A plot of the maximum width of the double ring sensor against the minimum depth at which photo acoustic signal has to be detected for peak to peak time of 25 ns.

Taking an inner radius of 2.0 mm and a width of the ring of 0.17 mm, then photo acoustic signals with a peak to peak time of 67 ns can be detected with maximum charge generation for depths larger than 7.5 mm. Besides influencing the maximum charge generation, also the width of the ring determines the broadening of the peak to peak time of the detected signals, as there will be interference of the acoustic waves, arriving at the ring shaped sensor surface. To improve the directional sensitivity of the ring-shaped sensor, two rings can be used. The effect that the directional sensitivity does not decrease very rapidly to zero can be reduced using cross-correlation techniques. Furthermore, if a side-lobe occurs in the directional sensitivity this is related to the radius of the ring. As the second ring has a different radius, the side-lobe will appear at a different lateral displacement of the source. By simply adding the signals of both rings, the effect of side-lobes will already decrease with a factor 2.

3.4. Double Ring Sensor

Based on the described calculations of the sensor characteristics a double ring photo acoustic sensor was constructed. It consists of two concentric ring shaped sensor areas. The inner ring has an inner radius of 2 mm and a width of 0.17 mm. The outer ring has an inner radius of 3.5 mm and a width of 0.1 mm, so that the area of both rings is equal. This sensor will be capable of detecting photo acoustic signals with a peak to peak time of 67 ns, located at depths larger than 7.5 mm, without any significant distortion of the signals. The illumination system is integrated within the sensor module. The electrodes are constructed by using a printed circuit board (PCB) with two concentric copper circles (electrodes) on it. A metal hole through the PCB connects the electrodes to the amplifiers. The piezoelectric material is glued to the PCB, using significant pressure to minimize the thickness of the glue layer. Everything is embedded in a brass housing to shield the electronics for electromagnetic noise.

With increasing depth, also signals with a smaller peak to peak time can be detected undistorted. Furthermore, for photo acoustic signals with a peak to peak time larger than 67 ns, the minimum depth at which they are detected as being undistorted decreases further below 7.5 mm with increasing peak to peak time. In many applications of the sensor, there will be a distance between the tissue and the sensor of a few millimeters, which will be filled with ultrasound contact gel. So the effective depth (depth in the tissue) at which the signals can be located as being undisturbed is even smaller. For application of this sensor for monitoring the blood content in the brain, the minimum depth of interest is determined by the thickness of the skin, skull, and the cerebrospinal fluid layer. This total thickness is at least several mm. So the limitation on the minimum depth at which the sensor can measure photo acoustic signals undisturbed will not be a problem. The depth response of the two separate rings has been calculated for a spherical photo acoustic source, which generates an acoustic signal with a peak to peak time of 67 ns. The single sensor module has been diagrammatically depicted in Fig. 6. The lateral view is shown in Fig. 7. The sensor has been tested under different skin parameters. The perfect quantization ratio required for the skin layers and the skin densities have been maintained.

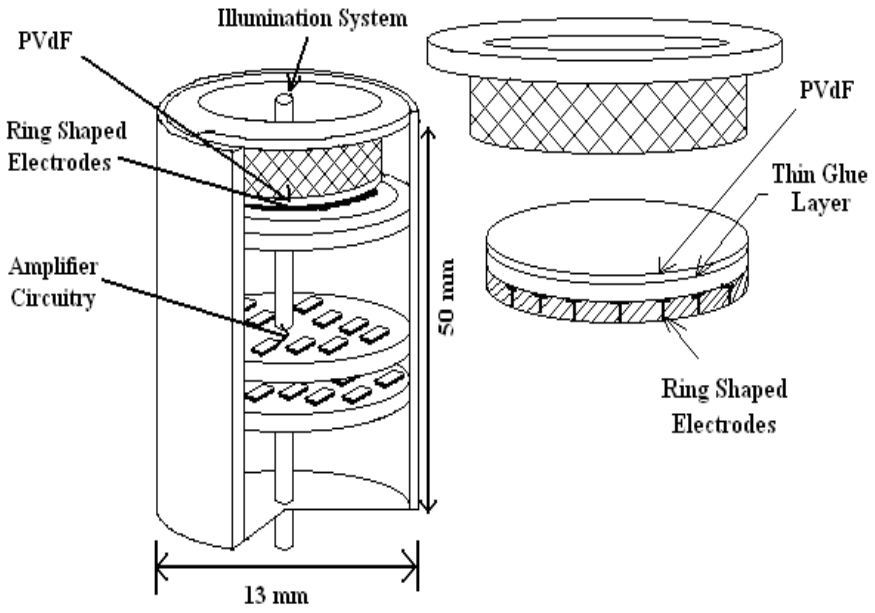

Fig. 6. The different components and layers of the double ring sensor.

Optical methods for detection of acoustic waves have been developed as well [1, 5, 11, 25].

But as broadband piezoelectric sensors are easier to construct and have a slightly better sensitivity than optical detection systems, the piezoelectric sensors are the best choice for this application. The maximum width of the ring is determined by the minimum depth at which the photo acoustic signal has to be detected with maximum charge generation.

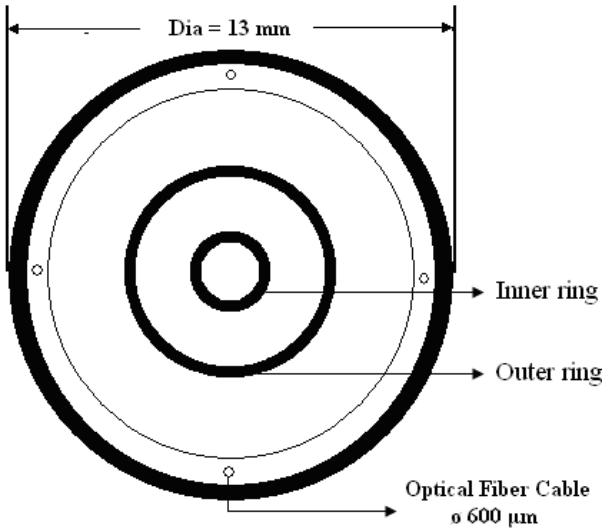

Fig. 7. Lateral view of the double ring sensor module with the ring type illumination system.

For instance, as mentioned taking an inner radius of 2.0 mm, and a width of the ring of 0.17 mm, then photo acoustic signals with a peak to peak time of 67 ns can be detected with maximum charge generation for depths larger than 7.5 mm. The model when tested with the phantom fingers brought out with maximum sensitivity. So the sensor model has been designed on a ring to fit in any one of the fingers in the real time model. The most common piezoelectric polymer is poly vinylidene fluoride (PVDF), which is available in different thicknesses ranging from 5 to 100 µm as a transparent film or coated with metals for electrical contact [21].

In the currently used pulsed PA analysis of the blood components through the skin, the generated pressure pulses are often detected in backward mode, where excitation and detection are performed at the same side of the sample. Since piezoelectric transducers are generally not transparent, illumination through the piezo and detection at the same point are not possible. This has been overcome by using the sensor set-up shown in the Fig. 8 and Fig. 9.

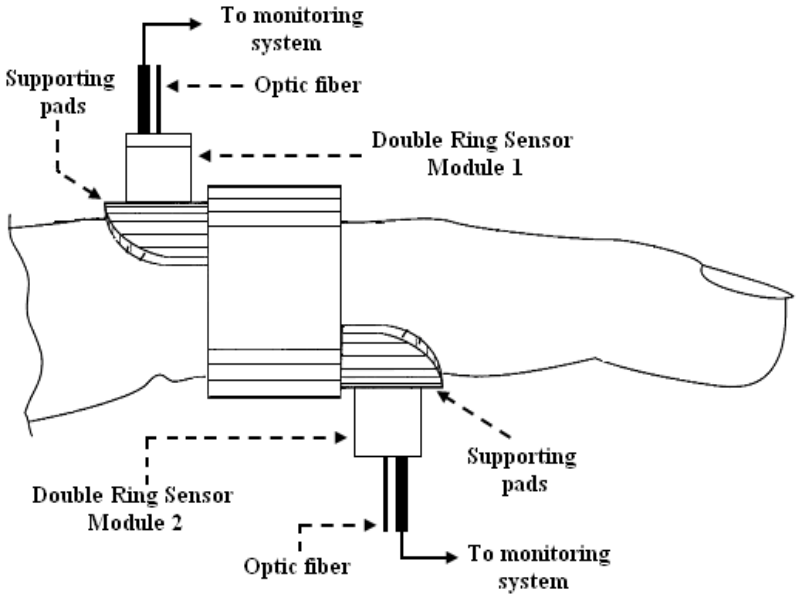

Fig. 8. Basic design for the technique in discussion.

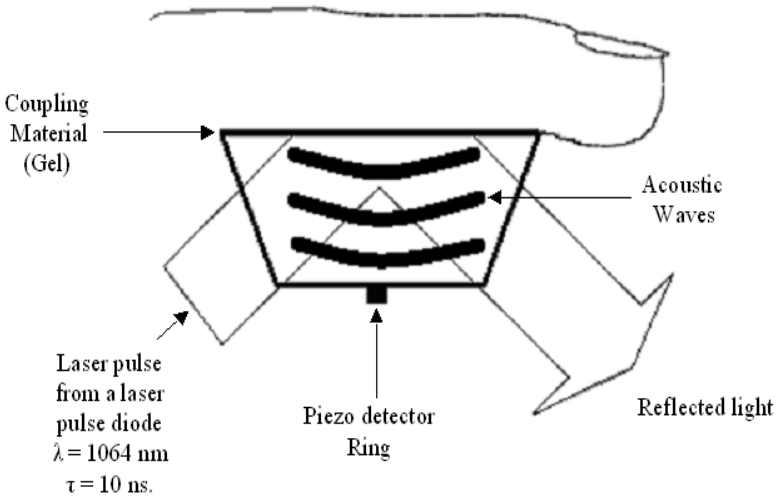

Fig. 9. Photo acoustic transducer model.

This PA sensor uses a transparent prism as coupling material for both illumination of the sample and transfer of the acoustic energy to the detector. The sample is eliminated through a transparent prism which also acts as an acoustic coupling material.

4. Signal Processing

In the near infrared, the scattering coefficient of the skin is much larger than its absorption coefficient. A collimated light beam at normal incident on a sufficiently thick skin can be considered. Assuming that the scattering and absorbing centers are uniformly distributed and neglecting internal light generation by fluorescence, the optical distribution can be described by the stationary radiative transfer equation, when the duration of a light pulse is longer than 10-8 ns.

$$s.\nabla I(r,s) = -\mu e\, I(r,s) + (\mu e / 4\pi) \int_{4\pi} p_f(s,s')\, I(r,s')\, d\omega + (\mu_e / 4\pi)\, p_f(s,z)\, I_c(r,z) \tag{3}$$

The collimated light is attenuated according to modified Beer's law, i.e.

$$d\int c(r,z) = -\mu_e I_c(r,z).dz, \tag{4}$$

where Ic(r, z) is the collimated intensity at the position r in the incident direction z, and r is a position vector. I(r, s) is the scattered specific intensity (watt/cm^2/sr) at the position r in the direction s, and s is the directional unit vector. $P_f(s,s')$ is the phase function that represents the scattering contribution from s' in the direction s. ω' is the solid angle μ_e is the extinction coefficient defined as the sum of the absorption coefficient μ_a and the scattering coefficient μ_s.

A powerful photo acoustic technique, to be precise, the Time-Resolved Stress Detection (TRSD) can be used to measure the absorption and scattering coefficients together and to image the interior structure of turbid samples. Since pressure is also an important factor the PA pressure of a planar PA source produced in a clear (non- scattering) absorbing medium by a short laser pulse (δ pulse) can be described by the equation.

$$p_a(\tau) = \{E_0\alpha\beta v^2 / 2C_p\}\{\Theta(-\tau).\exp(\alpha v_a\tau) + R_c\,\Theta(\tau) \exp(-\alpha v_a\tau)\} \tag{5}$$

$$p_t(\tau_t) = \{E_0\alpha\beta v^2 / 2C_p\}T.\Theta(\tau_t)\exp(-\alpha v_a\tau_t),$$

where

$$\begin{aligned} R_c &= (p_t v_t - p_a v_a)/(p_t v_t + p_a v_a) \\ T &= 2p_t v_t/(p_t v_t + p_a v_a) \\ \tau &= t-(z/v_a) \\ \tau_t &= t+(z/v_t) \end{aligned} ;$$

Θ is the Heaviside unit function; ρ and v are the density and the acoustic velocity of the medium, respectively. The subscripts a and t describe the parameters in the absorbing and the transparent media. At initial time (t = 0), when the laser incidents on the absorbing medium, the above equation is simplified as

$$P(z) = (E_0\alpha\beta v^2 / C_p)\exp(-\alpha z) = \Gamma E_0\alpha\exp(-\alpha z) \tag{6}$$

But the tissues and cells cannot be considered as non-scattering medium and hence considering the reduced scattering coefficient of the tissues μ_s' to be much larger than its absorption coefficient μ_a the corresponding stress can be modified as

$$\begin{aligned} P(0) &= \Gamma E(0)\mu_a \qquad (z=0) \\ P(z) &= \Gamma E_0 K_s \mu_a \exp(-\mu_{eff} z) \\ &= (1/2)\Gamma E_0 \mu_{eff}(\exp(\mu_{eff} l^*) \\ &\quad -\exp(-\mu_{eff} l^*(2\Delta + l))\}\exp(-\mu_{eff} z). \end{aligned} ,$$

where $z > (1/\mu_{eff})$.

For optically thick samples, $E(0) = (1 \pm 7.1R_{d\infty})E_0$, where $R_{d\infty}$ is the total diffuse reflectance. K_s is the factor that accounts for the effect of backscattered irradiance that increases the effective energy density absorbed in the subsurface.

$$\begin{aligned} &M + h\upsilon \longrightarrow M^* + \Delta V_{el} ; \\ &M^* \xrightarrow[\tau]{} M + q ; \\ &M^* \xrightarrow{\tau'} + q' \xrightarrow{t''} P + q'' \\ &M^* \longrightarrow 1 + q' + \Delta V mol \\ &M^* \longrightarrow M + q'' + h\upsilon , \end{aligned}$$

where hυ - Energy Absorbed
ΔV_{el} - Volumetric Change
τ, τ', τ'' - Time Constants
P - Product after τ''

q - Released heat
hυ' - Released energy
and $\lambda = 1064$ nm; $\tau = 10$ ns

The acoustical pressure generated is

$$P(r,t) = 1/4\pi c * \partial/\partial t \left\{ \int [P_0(r - \Delta v)/ct] ds \right\}, \quad (7)$$

where P(r, t) is a function of radius and time.
Also

$$\partial^2/\partial t^2 P(r,t) - C^2 \nabla^2 P(r,t) = \partial/\partial t \; P_0(r) \partial(t),$$

where

$$P_0(r) = B\beta/C_p \, F_0 \mu_a \; \exp[-z\mu_a f(x)];$$

$\Delta r = ct$
where t - 10ns (from above)
c - Speed of sound 320 m / sec
C - Specific heat at constant volume
B - Bulk modulus (isothermal)

$$F(z) = F_0 \exp(-z\mu_a)$$

where z - depth
F_0 - Fluency at surface
μ_a - absorption

5. Results and Discussion

The real time demo model has been tested with 20 blood samples both in the diabetic range and the non diabetic range and they are satisfactory. The major implications and deductions from the output are plotted and the graphs have been illustrated here with the inferences. To assess the feasibility of photo acoustic noninvasive blood glucose detection, the technique was first used for in vitro studies in the mid-infrared region with aqueous glucose solutions and human whole blood [19]. With technique in discussion, using the described measurements of the sensor and an illumination system with a pulsed laser diode with pulse duration of 5-15 ns and at a repetition rate of 10 Hz, the glycated hemoglobin gave a peak at 1064 nm with the peak amplitude of the photo acoustic signal varying with the glycation of the hemoglobin.

5.1. Photo Acoustic Signal vs. Time

The input excitation pulse for the present technique is varied for 3 wavelengths viz. 790 nm, 960 nm and 1064 nm and corresponding acoustical amplitudes are together plotted (Table 2). The blood glucose concentration of a normal person (7 % HbA1c) is previously measured with the in-vitro techniques like the HPLC test. The analysis of the blood glucose concentration of the same person by this technique gave the output plot as shown below. The peaks are shown for the different wavelength

pulses in the Fig. 10. The graph gives an implication of a low peak for 1064 nm input pulse excitation which corresponds to the HbA1c. It is observed that the acoustic signals induced in the tissue start at around 2.25 μs, representing the time of flight of acoustical waves from the arteries to the sensor surface.

Table 2. Experimental Values.

Photo Acoustic Signal Strength (v)			**Distance (mm)**	**Time (μs)**
790 nm	**960 nm**	**1064 nm**		
0.13	0.09	0.04	0.75	0.5
0.24	0.11	0.03	1.3	0.9
0.17	0.08	0.02	1.5	1
-0.04	0.001	0.002	2.3	1.5
-0.01	-0.01	-0.01	3	2
0.39	0.55	0.15	3.7	2.3
-0.15	-0.26	-0.09	4.6	3.1
-0.05	-0.09	-0.001	6	4
-0.03	-0.03	-0.001	7.3	4.8

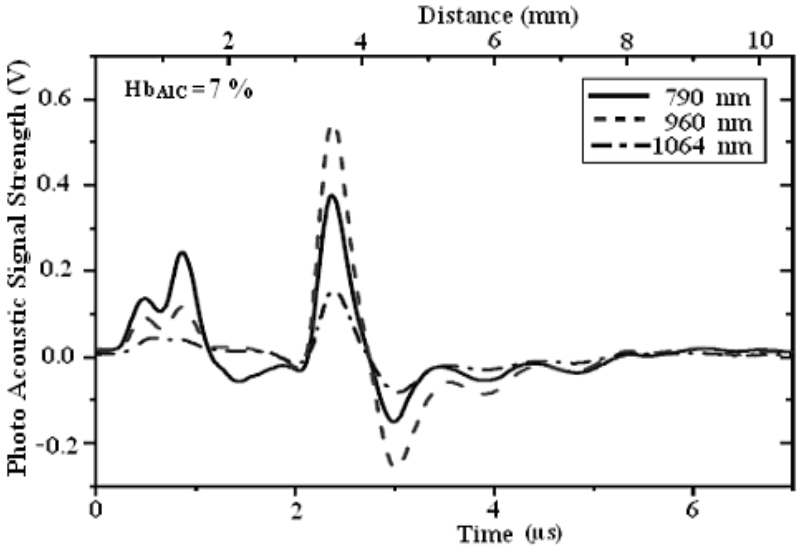

Fig. 10. A plot of PA amplitude against time for different input pulses given by a laser diode.

The above graph is used to formulate a standard photo acoustic model of the HbA1c molecule (stable Amadori rearranged ketoamine adduct).

5.2. Variations for Different Concentrations

The plot of the acoustical signals Vs time for different concentrations of glycated hemoglobin is shown in Fig. 11.

The photo acoustic signals induced in the blood start about 2 to 2.25 μs. This depends on the concentration of the glucose or the glycated hemoglobin. The first two peaks are the noise signal induced and detected by the detector system. These are not considered for any calculation purposes. Depending on the thickness of the skin there is a time shift in the signals induced and this is observed

in the graph plotted. The plot in Fig. 11 clearly indicates a change in the peak value with a change in the glycated hemoglobin concentration. The peak for a normal person (7%) is about 150 mV or 0.15 V. The plot is shown for four samples from among 20 patients who were tested. A 5 % indicates a non-diabetic person while that greater than 7 % is a diabetic patient. Once the signals are obtained the photo acoustic slope is calculated from the recorded signals and the slope is found to be linearly increasing with the glycated hemoglobin concentration. The Fig. 12 shows this plot.

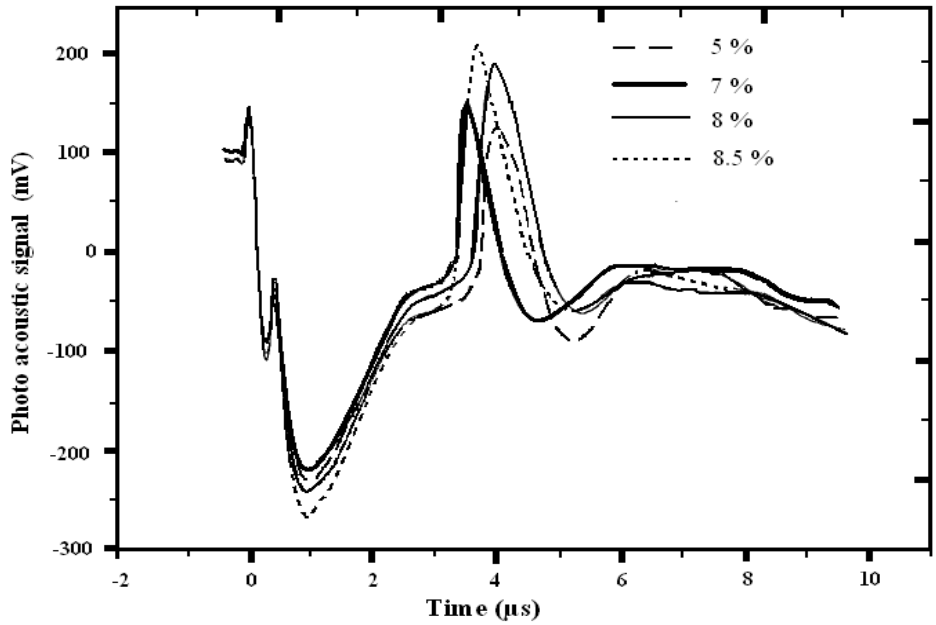

Fig. 11. Plot of photo acoustic signal Vs time for different percentages of glycated hemoglobin.

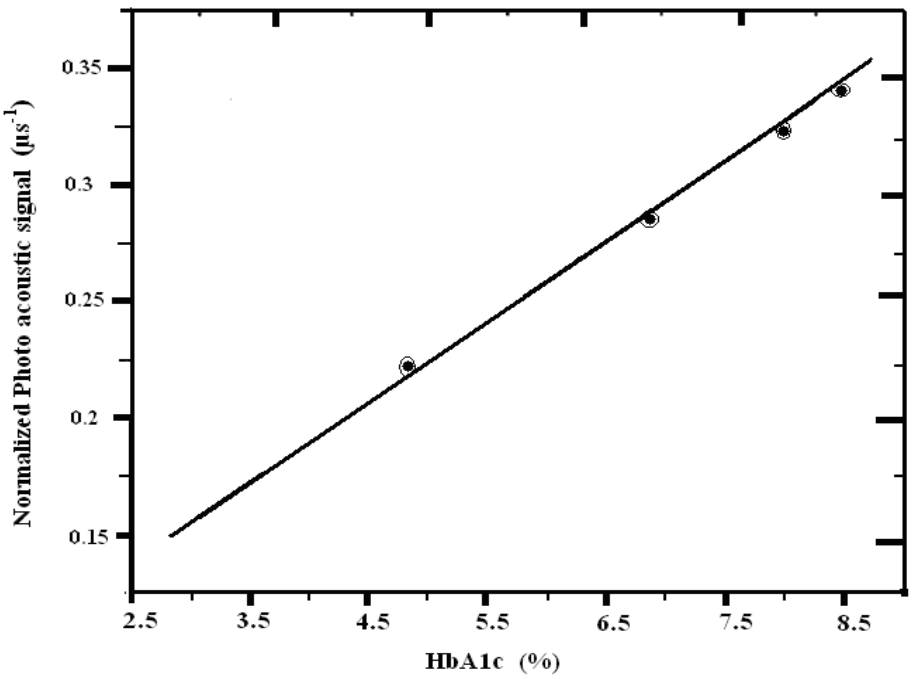

Fig. 12. Plot of normalized photo acoustic signal Vs different percentages of glycated hemoglobin.

The plot above indicates the four values of glycated hemoglobin among the 20 samples for which the testing is carried out. Before the calculation of the slope the signals are normalized. This is done in order to provide high efficiency (glycated hemoglobin % from 1-15 % is clearly detected).

5.3. Frequency Analysis

As mentioned the frequency ranges from 1-75 MHz are monitored with an established center frequency at 22 MHz. The bandwidth model of the filter is shown in Fig. 13.

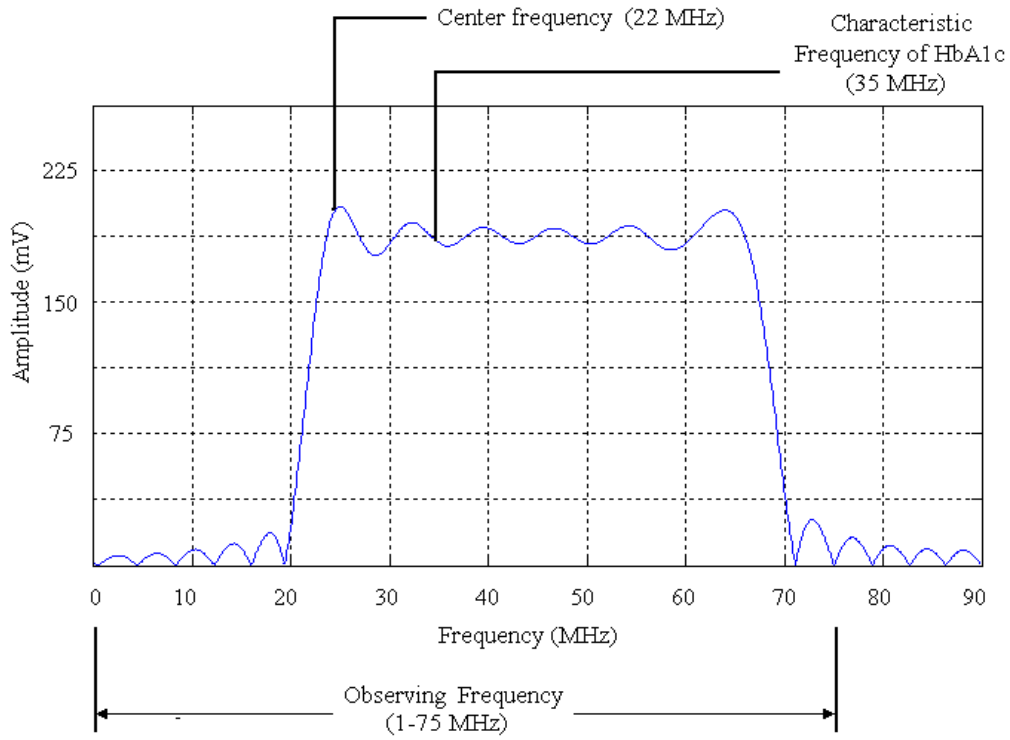

Fig. 13. Bandwidth of the filter.

The glycated hemoglobin frequency is estimated to be at about 35 MHz. This is the characteristic frequency output observed for the HbA1c molecule. The filters are also designed to filter out all other frequencies other that those from ±10 of the HbA1c frequency. This is then carried out for sampling and the individual signals extracted. The pressure profile of the stress variation can also be obtained, from which various parameters including the glycated hemoglobin concentration is quantified. This is discussed in the next section

5.4. Determination of Hba1c Concentration from the Obtained Signals

The HbA1c concentration (%) is calculated by the various sampling processes and sorting out of the characteristic peak by analyzing the pressure profile. This is, as mentioned, dependent on the absorption coefficient of the medium (tissue, skin and blood). The absorption coefficient is used here to quantify the glycated hemoglobin. The various aspects of the absorption coefficient with the photo acoustic signals are discussed here.

5.5. Absorption Coefficient vs. Hba1c

By knowing the absorption coefficient and the molar extinction coefficient e, the glycated hemoglobin concentration is easily calculated. The absorption coefficient of the tissues and skin are related to the glycated hemoglobin concentration and these have been plotted as shown in Fig. 14.

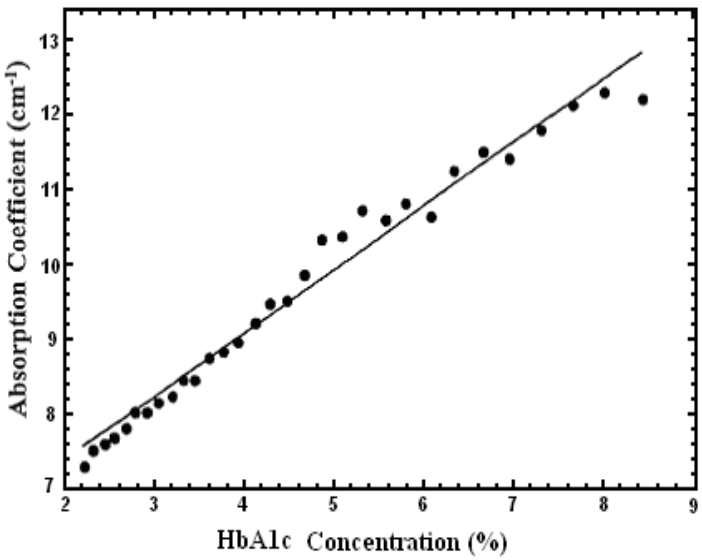

Fig. 14. Absorption Coefficient Vs Hba1c.

It is observed from the above plot that the variation of the hemoglobin concentration comes in a linear manner with the absorption coefficient. Though there is a slight deviation from the actual values, these results are acceptable for practical purposes.

5.6. Resultant Plot (Hba1c (%) vs. PA Signal)

Since the variation of photo acoustic signal strength with the absorption coefficient is known and the variation of the absorption coefficient with the glycated hemoglobin is also known, a correlation between the variations of photo acoustic signal strength with the glycated hemoglobin concentration is made. The resultant HbA1c concentration is thus determined from the photo acoustic output variation and when plotted on a single sheet gave the graph shown in Fig. 15. It is observed that there is a one to one relationship between the photo acoustic signal strength and the HbA1c concentration. Though the plot is not perfectly linear, it shows a good interpretation of particular photo acoustic signal values.

For example, the photo acoustic signal of strength of 0.15 V or 150 mV corresponds to glycated hemoglobin percentage of 7 %.

5.7. Comparison with a Standard In-vitro Technique

After obtaining the glycated hemoglobin percentage values through the model discussed in this work, the results are verified by comparing with a standard in vitro technique. The HPLC test is one of the commonly followed in-vitro techniques for blood glucose determination. This test has been taken as the standard in this work. The patients are first tested with the regular in vitro HbA1c test and the percentage HbA1c is quantified. The percentage is again calculated using the technique discussed here

and the comparative chart in the one shown in Fig. 16. The following graph shows the result comparison of the above technique with the standard HPLC test.

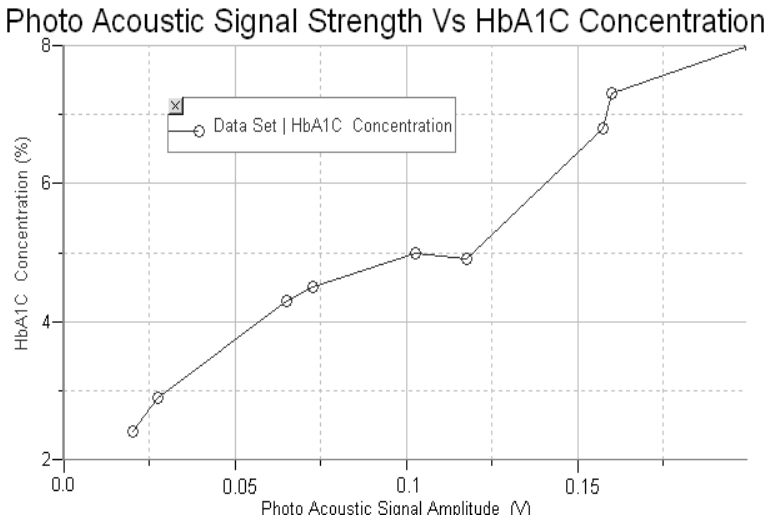

Fig. 15. Photo acoustic signals plotted against the HbA1c (%) values.

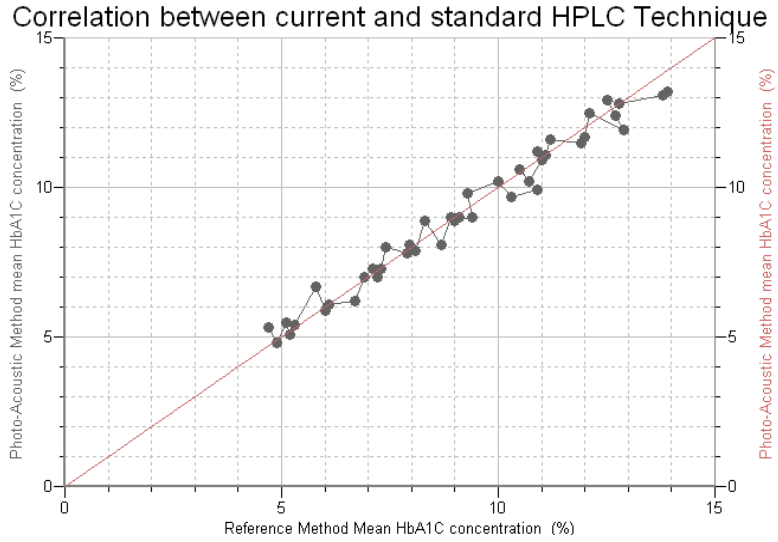

Fig. 16. Correlation between current and standard HPLC technique.

It is observed from the graph that this method has only a slight variation with respect to the in vitro techniques and thus is very reliable. The errors and their rectification methods and other factors have been presented in the next section. The glycated hemoglobin percentage values of different patients are plotted in a comparison.

The error obtained by this technique does not stand with the Raman Spectroscopy. In Raman spectroscopy the concentration of glucose is measured directly meaning in the blood. Thus this result varies before and after food and other conditions. But this research proposes a model wherein the results shows the concentration of glycated hemoglobin which does not vary with such conditions. The measurement of glycated hemoglobin using photo acoustic technique in this research has been a novel approach, the first of its kind, in glucose quantification (glycated hemoglobin). This technique has an error percentage of around 9%. This is observed from the graph plotted in Fig. 16. It can be made more

efficient using the photo acoustic spectroscopy. The cost functions and the performance functions have been defined and stand good. The graphical results have been stated by testing the instrument under different conditions and results have been found satisfactory.

References

[1]. Bell A. G., On the production and reproduction of sound by light, *Am. J. Sci*., Vol. 20, 1880.

[2]. Brownlee M., Negative consequences of glycation, *Metabolism*, 49, Suppl. 1, 2000, pp. 9-13.

[3]. Brownlee M., Cerami A., Vlassara H., Advanced products of non enzymatic glycosylation and the pathogenesis of diabetic vascular disease, *Diabetes Metab Rev.,* 4, 5, 1988, pp. 437-451.

[4]. Chandalia H. B. and Krishnaswamy P. R., Glycated hemoglobin, *Current Science,* Vol. 83, No. 12, 25 December, 2002, pp 1522-1531.

[5]. Crum L. A. and Roy R. A., *Sonoluminescence, Science*, Vol. 266, No. 5183, 1994, pp. 233 – 234.

[6]. Diebold G. J. and Sun T., Properties of photoacoustic wave in one two and three dimensions, *Acustica*, Vol. 80, 1994, pp. 339-351.

[7]. Edward Profio A., Light transport in tissue, *Appl Opt*., Vol. 28, Issue 12, June 15, 1989, pp. 2216- 2222.

[8]. Fischbacher C., Jagemann K. U., Danzer K., Muller U. A., Papenkordt L. and Schuler J., Enhancing calibration models for non-invasive near-infrared spectroscopical blood glucose determination, *Fresenius J. Anal. Chem*., Vol. 359, Issue 1, 1997, pp. 78-82.

[9]. Freeborn S. S., Hannigan J., Greig F., Suttie R. A. and MacKenzie H. A., A pulsed photo acoustic instrument for the detection of crude oil concentrations in produced water, *Rev. Sci. Instrum*., Vol. 69, No. 11, November, 1998, pp. 3948-3952.

[10]. Griffiths P. R., Infrared emission spectroscopy. I. Basic considerations, *Appl. Spectrosc*., Vol. 26, Issue 1, 1972, pp. 73-76.

[11]. Hoelen C. G. A., de Mul F. F. M., Pongers R. and Dekker A., Three dimensional photoacoustic imaging of blood vessels in tissue, *Opt. Lett*., Vol. 23, 1998, pp. 648-650.

[12]. H. Vlassara, H Fuh, Z. Makita, S. Krungkrai, A. Cerami, R. Bucala, Exogenous advanced glycosylation end products induce complex vascular dysfunction in normal animals: a model for diabetic and aging complications, *Proc Natl Acad Sci U S A*., 89, 24, December 15, 1992, pp. 12043–12047.

[13]. Ishimaru A., Diffusion of light in turbid material, *Appl. Opt*., Vol. 28, 1989, pp. 2210-2215.

[14]. Jackson W and Amer N. M., Piezoelectric photoacoustic detection: Theory and experiment, *J. Appl. Phys*., Vol. 51, 1980, pp. 3343-3353.

[15]. Jean-Luc Wautier, P. J. Guillausseau, Diabetes, advanced glycation end products and vascular disease, *Vascular Medicine*, Vol. 3, No. 2, 1998, pp. 131-137.

[16]. Lane M. D. and Christensen P. R., Thermal infrared emission spectroscopy of anhydrous carbonates, *J. Geophys. Res*., Vol. 102, No. E11, 1997, pp 25581-25592.

[17]. McCance D. R, Dyer D. G, Dunn J. A, Bailie K. E, Thorpe S. R, Baynes J. W, Lyons T. J, Maillard reaction products and their relation to complications in insulin-dependent diabetes mellitus, *J. Clin. Invest.,* 91, 1993, pp. 2470-2478.

[18]. Petrova I. Y., Prough D. S., Petrov Y. Y., Brecht H. -P. F., Svensen C. H., Olsson J., Deyo D. J., Esenaliev R. O., Optoacoustic technique for continuous, noninvasive measurement of total hemoglobin concentration: an in vivo study, Engineering in Medicine and Biology Society, IEMBS apos 04, in *Proceedings of 26th Annual International Conference of the IEEE*, Vol. 1, 1-5 Sept., 2004, pp. 2059 – 2061.

[19]. Quan K. M., Christison G. B., MacKenzie H. A. and Hodgson P., Glucose determination by a pulsed photoacoustic technique using a gelatin based phantom, *Phys. Med. Biol*., Vol. 38, 1993, pp. 1911-1922.

[20]. Seetharama Acharya A. and Manning J. M., Amadori Rearrangement of Glyceraldehyde-Hemoglobin Schiff Base Adducts, *Journal of Biological Chemistry*, Vol. 255, No. 15, 1980, pp. 7218-224.

[21]. Sessler G. M., Piezoelectricity in Polyvinylidenefluoride, *J. Acoust. Soc. Am*., Vol. 70, Issue 6, 1981, pp. 1596-1608.

[22]. Shults M. C., Rhodes R. K., Updike S. J., Gilligan B. J. and Reining W. N., A telemetry instrumentation system for monitoring multiple subcutaneously implanted glucose sensors, *IEEE Transactions on Biomedical Engineering*, Vol. 41, 1994, pp. 937-942.

[23]. Sternberg F., Meyerhoff C., Mennel F. J., Bischof F. and Pfeiffer E. F., Subcutaneous glucose concentration: its real estimation and continuous monitoring, *Diabetes Care*, Vol. 18, 1995, pp. 1266-1269.

[24]. S. R. Thorpe, J. W. Baynes, Role of the Maillard reaction in diabetes mellitus and diseases of aging, *Drugs Aging*, 9, 1996, pp. 69-77.
[25]. Tam C Andrew, Applications of photoacoustic sensing techniques, *Rev. Mod. Phys*., Vol. 58, 1986, pp. 381-431.
[26]. Thomas J. Allen and Paul C. Beard, Pulsed near-infrared laser diode excitation system for biomedical photo acoustic imaging, *Opt. Lett.*, Vol. 31, No. 23, December 1, 2006.
[27]. Vlassara H., Brownlee M., Cerami A., Nonenzymatic glycosylation: role in the pathogenesis of diabetic complications, *Clinical Chemistry*, 32, 10 Suppl, 1986, pp. B37-41.
[28]. Welch A., The thermal response of laser irradiated tissue, *IEEE Journal of Quantum Electronics*, Vol. 20, Issue 12, Dec, 1984, pp. 1471 – 1481.
[29]. Wilson E. B., Decius J. C. and Cross P. C., Molecular vibrations: The theory of infrared and Raman vibrational spectra, *McGraw-Hill*, New York, 1955.
[30]. X. Dou, Y. Yamaguchi, H. Yamamoto, H. Uenoyama, and Y. Ozaki, Biological Applications of Anti-Stokes Raman Spectroscopy: Quantitative Analysis of Glucose in Plasma and Serum by a Highly Sensitive Multichannel Raman Spectrometer, *Appl. Spectrosc*. 50, 1996, pp. 1301-1306.

Guide for Contributors

Aims and Scope

Sensors & Transducers Journal (ISSN 1726-5479) provides an advanced forum for the science and technology of physical, chemical sensors and biosensors. It publishes state-of-the-art reviews, regular research and application specific papers, short notes, letters to Editor and sensors related books reviews as well as academic, practical and commercial information of interest to its readership. Because it is an open access, peer review international journal, papers rapidly published in *Sensors & Transducers Journal* will receive a very high publicity. The journal is published monthly as twelve issues per annual by International Frequency Association (IFSA). In additional, some special sponsored and conference issues published annually.

Topics Covered

Contributions are invited on all aspects of research, development and application of the science and technology of sensors, transducers and sensor instrumentations. Topics include, but are not restricted to:

- Physical, chemical and biosensors;
- Digital, frequency, period, duty-cycle, time interval, PWM, pulse number output sensors and transducers;
- Theory, principles, effects, design, standardization and modeling;
- Smart sensors and systems;
- Sensor instrumentation;
- Virtual instruments;
- Sensors interfaces, buses and networks;
- Signal processing;
- Frequency (period, duty-cycle)-to-digital converters, ADC;
- Technologies and materials;
- Nanosensors;
- Microsystems;
- Applications.

Submission of papers

Articles should be written in English. Authors are invited to submit by e-mail editor@sensorsportal.com 6-14 pages article (including abstract, illustrations (color or grayscale), photos and references) in both: MS Word (doc) and Acrobat (pdf) formats. Detailed preparation instructions, paper example and template of manuscript are available from the journal's webpage: http://www.sensorsportal.com/HTML/DIGEST/Submition.htm Authors must follow the instructions strictly when submitting their manuscripts.

Advertising Information

Advertising orders and enquires may be sent to sales@sensorsportal.com Please download also our media kit: http://www.sensorsportal.com/DOWNLOADS/Media_Kit_2008.pdf